

Influence of high pressure on the luminescence transitions of Mn⁴⁺-doped gadolinium gallium garnet

This article has been downloaded from IOPscience. Please scroll down to see the full text article.

2005 J. Phys.: Condens. Matter 17 7185

(<http://iopscience.iop.org/0953-8984/17/46/003>)

View [the table of contents for this issue](#), or go to the [journal homepage](#) for more

Download details:

IP Address: 129.252.86.83

The article was downloaded on 28/05/2010 at 06:45

Please note that [terms and conditions apply](#).

Influence of high pressure on the luminescence transitions of Mn⁴⁺-doped gadolinium gallium garnet

D Galanciak¹, M Grinberg², W Gryk², S Kobayakov³, A Suchocki³,
G Boulon⁴ and A Brenier⁴

¹ Department of Physics, University of Bydgoszcz, Weyssenhoffa 11, 85-072 Bydgoszcz, Poland

² Institute of Experimental Physics, Gdansk University, ulica Wita Stwosza 57, 80-952 Gdansk, Poland

³ Institute of Physics, Polish Academy of Sciences, Aleja Lotników 32/46, 02-668 Warsaw, Poland

⁴ Physical Chemistry of Luminescent Materials, Claude Bernard/Lyon I University UMR 5620CNRS, Batiment A Kastler, 10 Rue AM Ampere, 69622 Villeurbanne, France

Received 28 June 2005, in final form 8 September 2005

Published 1 November 2005

Online at stacks.iop.org/JPhysCM/17/7185

Abstract

We present results of a high-pressure photoluminescence study of Mn- and Ca-doped gadolinium gallium garnet (GGG) crystals. Since the Mn⁴⁺ ion has the same electronic structure of the open 3d³ shell as Cr³⁺, its spectroscopic properties are expected to be similar to those of the Cr-doped GGG. We observed the luminescence R-lines of various Mn⁴⁺ centres in GGG. In the 0–118 kbar pressure range those R-lines shift linearly to lower energies. The pressure coefficients are of the order of 2 cm⁻¹ kbar⁻¹, about three times larger than that for Cr³⁺ ions. This fact can be explained by different strength of coupling of isoelectronic Cr³⁺ and Mn⁴⁺ ions with GGG host. The changes of the radiative decay times of the Mn⁴⁺ centres as a function of pressure are fitted with a theoretical model.

1. Introduction

The Gd₃Ga₅O₁₂ garnets (GGGs) with various dopants are interesting for applications in the field of solid-state laser materials. Especially important in this field are GGG crystals doped with some rare-earth dopants such as Nd or Er. Also the optical properties of Mn-doped crystalline materials are of continuing interest for these applications. Many interesting properties of those crystals remain yet not well explained in spite of several studies of these systems that have already been performed (Donegan *et al* 1986, Suchocki *et al* 1986, Brenier *et al* 1992, Moncorge *et al* 1994, Stoyanova *et al* 2000, Zheng 1999, Loutts *et al* 1988, Hazenkamp *et al* 1997, Geschwind *et al* 1962, Hernandez *et al* 1999, Jovanić 1997).

Garnet crystals have general chemical formula C₃A₂D₃O₁₂, where C denotes dodecahedrally, A octahedrally and D tetrahedrally coordinated crystallographic sites (Sturve and Huber 1985). Although perfect garnet structure is cubic, garnet crystals with chemical formula C₃B₅O₁₂ exhibit distortions from cubic symmetry due to partial exchange of sites

between C and B atoms (Dong and Lu 1991). Mn^{4+} in GGG replaces Ga^{3+} ion the octahedral sites. Since Ga^{3+} is trivalent, it is necessary to compensate for the charge discrepancy by co-doping of the material with divalent cations. Ca^{2+} ions were used for charge compensation in the crystals studied in this work. The Ca^{2+} ions in the GGG host are located in the dodecahedral Gd^{3+} sites. The charge-compensating ions may further lower the symmetry of the particular crystallographic sites.

Mn^{4+} ion has the same electronic configuration $3d^3$ as Cr^{3+} . The energetic structure of this ion is well described by standard crystal-field theory (Sugano *et al* 1970). The sequence of energy levels is determined by the symmetry of ion site, by the crystal-field strength $10Dq$ and by interelectronic interactions determined by the Racah parameters B and C . The crystal field strength $10Dq$ is equal to the energy difference between the 4A_2 and 4T_2 states and depends approximately on the fifth power of the metal–ligand distances, according to the point-charge crystal-field model.

The Mn^{4+} ions are located in the GGG host in the sites with octahedral symmetry (Brenier *et al* 1992). The energy structure of Mn^{4+} is in agreement with the Tanabe–Sugano diagram for d^3 electronic configuration in the so-called strong crystal field. The ground state is the 4A_2 , the lowest excited is 2E , and the first quartet 4T_2 state is located above the 2E state. Therefore the emission spectra are dominated by a sharp luminescence, the so-called R-lines. Due to the fact that ${}^2E \rightarrow {}^4A_2$ transitions are spin-forbidden, their decay times are in the millisecond range. The spin-allowed ${}^4T_2 \rightarrow {}^4A_2$ transitions are characterized by much shorter decay times, of the order of tenths of microseconds (Sugano *et al* 1970, Grinberg *et al* 1993, Grinberg and Orlikowski 1992).

There are two important effects that influence the spectroscopic properties of the dopant ions: electron–phonon coupling (it is significant in the case of the 4T_2 state and negligible in the case of 2E state) and the spin–orbit interaction, that allows the ${}^2E \rightarrow {}^4A_2$ transitions (Sturve and Huber 1985, Sugano *et al* 1970, Grinberg *et al* 1993, Grinberg and Orlikowski 1992). The spin–orbit interaction and trigonal field distortion cause the 2E state splitting. As a result, two R-lines (R_1 and R_2) instead of one are observed in the absorption and emission spectra.

We applied the high-pressure technique in order to obtain more information about Mn^{4+} centres in GGG and resolve the different centres of those ions. The effect of high pressure on the optical properties of Mn^{4+} in GGG, positions of the R-lines and their fluorescence lifetimes have not been investigated yet. High pressure reduces the distances between a dopant ion and its environment. Thus, it causes an increase of the strength of the crystal field experienced by dopant ions, allowing one to obtain the information about their electronic structure. According to previous studies (Hong *et al* 1996) the GGG crystals remains cubic under pressure up to about 860 kbar. Above this pressure amorphization occurs. Thus we assume that the cation–ligand distances change with pressure in those crystals in accordance with the proper equation of state.

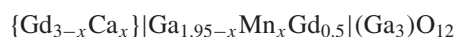
The effect of pressure on the 2E and 4T_2 states can be described in the cubic crystal-field approximation neglecting spin–orbit interaction and electron–phonon coupling (Loutts *et al* 1988). In this approximation the 4T_2 energy is proportional to the crystal-field strength parameter Dq . Thus the 4T_2 energy increases with increasing pressure. In contrast, the 2E energy remains nearly unaffected by pressure. Only a small red shift of the 2E energy is typically observed and it is attributed to a decrease of the interelectronic repulsion Racah parameters B and C with pressure—the so-called nephelauxetic effect. This effect is related to change of interelectronic repulsion of the d electrons due to increased covalency of the central ion–oxygen bonds with increased pressure. At a given temperature, the extent of thermal coupling between the 2E and the 4T_2 levels depends on the energy difference Δ between those

levels that can be controlled by varying the crystal-field strength of the host lattice. The energy difference Δ increases with increase of pressure since the crystal-field strength increases with pressure. The increase in the energy difference between ²E and ⁴T₂ states leads to the reduction and eventual elimination of the thermal population of the ⁴T₂ level.

The ²E and ⁴T₂ states may also be mixed by the spin-orbit interaction (Grinberg *et al* 1995). The extent of spin-orbit coupling also depends on Δ . The mixing due to this coupling is maximum for $\Delta = 0$ and decreases with the absolute value of Δ . As a consequence of thermal and spin-orbit coupling, the properties of the first excited state of Mn⁴⁺ reflect a combination of the properties of the ²E and ⁴T₂ levels. Since emission from the ²E state is spin forbidden, its lifetime is strongly influenced by admixture of the ⁴T₂ level. The reduction in spin-orbit coupling with increasing pressure leads to reduction in the mixing between the ²E and ⁴T₂ states. Thus increasing pressure causes an increase of lifetime of luminescence of the ²E state.

2. Experimental details

The GGG:Mn⁴⁺ crystals were grown by the Czochralski technique at Lyon I University. Manganese was added in the form of MnO₂. An equal quantity of charge-compensating Ca²⁺ ions was added to the melt in the form of CaCO₃. The starting composition of the melt was



with $x = 4.85 \times 10^{-3}$. The symbols { }, | and () stand, for dodecahedral, octahedral and tetrahedral sites, respectively.

Continuous-wave emission spectra were obtained using various lines of an argon-ion laser as the excitation source. The spectra were measured with use of GDM-1000 double-grating monochromator equipped with an EMI 9558B photomultiplier with S20-type cathode and an SR530 lock-in amplifier. The spectra were corrected for the quantum efficiency of the photomultiplier and throughput of the monochromator. The high-pressure measurements were performed with use of low-temperature diamond-anvil cell (Diacell Products MCDAC-1). The argon was used as a pressure-transmitting medium. The diamond-anvil cell was mounted into an Oxford 1204 cryostat equipped with temperature controller for low-temperature measurements. The R₁-line ruby luminescence was used for pressure calibration (Piermarini *et al* 1975, Noack and Holzapfel 1976). The polished samples of thickness of about 30 μm were loaded into the cell along with a small ruby ball. To measure the luminescence the argon-ion laser line was focused either on the measured GGG sample or on the ruby. The changes of pressure were made at room temperature in order to minimize non-hydrostatic effects that are known to exist in diamond-anvil cells especially at higher pressure. The hydrostatic conditions could be partially monitored by recording the half-width of the ruby emission. In our measurements we observed increase of the half-width of ruby luminescence with increasing pressure. The half-width of the R₁ ruby luminescence did not exceed 6 cm^{-1} at high pressures (2.5 cm^{-1} at ambient pressure). This means that the non-hydrostatic effects were rather weak.

The decay kinetics of the luminescence were measured with the use of an SR430 Multichannel Scaler. A large number of decays (typically a few tens of thousands) was collected in order to obtain good signal-to-noise ratio. The exciting laser beam was chopped by an acousto-optic modulator with the transient time below 10 ns or by mechanical chopper with transient time of below 10 μs . The decay kinetics were stored in the computer. The decay times of luminescence were calculated by fitting the decay kinetics with single- or double-exponential dependences.

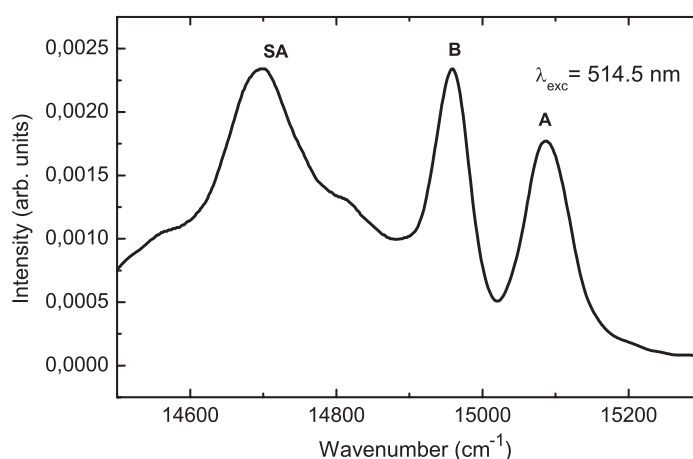


Figure 1. The luminescence spectrum in the region of the R lines of the GGG:Mn⁴⁺ crystal at ambient pressure, excited by a 514.5 nm argon-ion laser line at $T = 15$ K.

3. Experimental results

The luminescence spectrum of the GGG:Mn⁴⁺ crystal in the region of the R-lines, excited by the 514.5 nm argon-laser line at 15 K, is presented in figure 1.

This spectrum consists of two, relatively sharp lines at 663.5 nm (15 072 cm⁻¹) and 668.7 nm (14 955 cm⁻¹), labelled as A and B, respectively, and the broader structure, peaked at 681 nm (14 684 cm⁻¹) labelled as SA. The A and B lines (further considered as R_A and R_B line, respectively) are the zero-phonon R₁ lines from different Mn⁴⁺ sites in GGG in a relatively strong crystal field. The observed zero-phonon lines are broadened due to relatively large disorder caused by co-doping by charge-compensating Ca²⁺ ions. It was proved (Brenier *et al* 1992) that the broader structure about 681 nm is mostly associated with the A centre—it is a vibronic sideband of this centre.

The third minor centre, C, peaking at 671 nm (14 903 cm⁻¹), was observed in Brenier *et al* (1992). It was studied with the use of a spectrally resolved laser spectroscopy technique. In our case (figure 1) the C centre is not visible separately. The only effect of centre C is a relatively small shift of the position of the peak B (about 20 cm⁻¹) towards longer wavelength as compared with the spectral position of pure centre B (Brenier *et al* 1992). At the higher temperatures the luminescence spectra are more complicated and more difficult to resolve, mostly due to thermal population of the R₂ lines, which cause spectral overlap of luminescence from different Mn⁴⁺ centres.

The shape of the emission spectrum is determined by the excitation wavelength especially for higher pressures. In figure 2 we present the spectra of GGG:Mn⁴⁺ for different excitation at $T = 15$ K and at $P = 124$ kbar. Taking into account this effect we investigated our sample in the pressure range between 0 kbar and 150 kbar at $T = 15$ K, using excitation wavelengths 488 and 514.5 nm.

Our results are presented in figures 3(a) and (b), respectively. For the higher excitation energy (20 492 cm⁻¹–488 nm) the R_A line becomes dominant, but its sideband becomes weaker. That means that the A site appears to be more affected by Ca²⁺ ions at higher pressures. For the lower excitation energy the picture is the inverse: with increasing pressure the R_B line becomes dominant, and the R_A line is very weak.

Relative changes of the intensity of the A and B centres can be caused by two effects: (a) relative changes of the excitation efficiency at given excitation wavelength due to the pressure

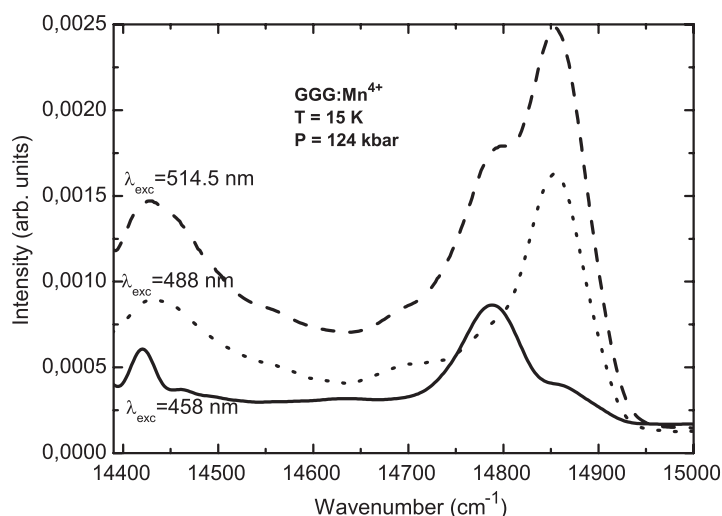


Figure 2. The excitation dependence of the luminescence spectra of the GGG:Mn⁴⁺ crystal at $T = 15$ K and $P = 124$ kbar.

shift of the ⁴T₂ bands to the higher energy, and (b) an increased contribution of electric-dipole-allowed transitions. Lack of detailed knowledge on the pressure dependence of the positions of the absorption spectra with pressure does not allow us to distinguish reliably between these two possibilities.

These observations are summarized in figure 4, where the relative integrated intensities of various luminescence lines (R_A, R_B, and SA) to the total luminescence intensity as a function of pressure are presented.

Spectral positions of the R_A and R_B lines as a function of applied pressure are presented in figure 5. The position of the R_A and R_B lines is approximately linearly pressure dependent, with pressure coefficients equal to $dE_A/dp = -1.87 \text{ cm}^{-1} \text{ kbar}^{-1}$ and $dE_B/dp = -1.49 \text{ cm}^{-1} \text{ kbar}^{-1}$, respectively. Note that the A site is more strongly affected by pressure than the B site.

In order to obtain more information about the A and B manganese centres in GGG, we investigated the decay kinetics of manganese luminescence excited at 514.4 nm, measured at the peaks of the emission of the centres A and B. These decay kinetics of Mn⁴⁺ are nearly single exponential with a decay time at 15 K and at ambient pressure equal to 1280 μs for the A centre, and 500 μs for the B centre, in agreement with previous results (Brenier *et al* 1992).

In figures 6 and 7 we show the effect of pressure on the luminescence lifetimes of the R_A and R_B lines of Mn⁴⁺:GGG. The decay times increase with increasing pressure for both centres.

4. Discussion

4.1. The effect of pressure of the luminescence spectra and luminescence lifetimes of the A and B Mn⁴⁺ centres

The sharp R-lines are associated with different Mn⁴⁺ centres, which have different environments in the GGG host. Replacing Ga³⁺ by Mn⁴⁺ ions in GGG crystal does not significantly deform the host lattice because the ionic radii of these ions are comparable, and equal to 62 and 60 pm, respectively. A similar case occurs if Ca²⁺ substitute Gd³⁺ ions (ionic radii: 99 and 94 pm, respectively). Therefore the difference between the sites may be mainly

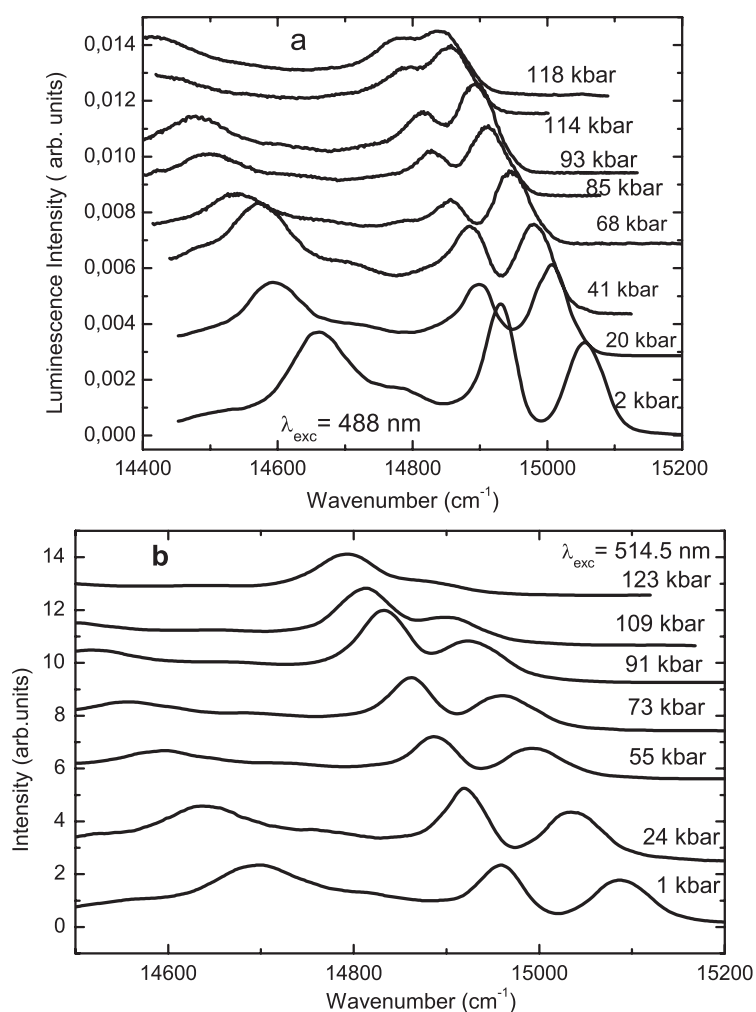


Figure 3. The influence of hydrostatic pressure on the luminescence spectra of the GGG:Mn⁴⁺ crystal excited by (a) 488 nm, (b) 514.5 nm argon-ion laser lines. The spectra were taken at $T = 15$ K.

due to the different distances of Ca²⁺ charge-compensating ions from the central Mn⁴⁺ ion. As was mentioned earlier, the Ca²⁺ ions are located in the dodecahedral sites. The shortest distance between dodecahedral and octahedral sites is almost two times smaller than the shortest distance between two octahedral sites. Thus the Mn⁴⁺ centres can be strongly affected by the presence of the Ca²⁺ ions.

It was seen (Brenier *et al* 1992) that the broader structure about 681 nm is mostly associated with the A centre—it is a vibronic sideband of this centre. Its intensity is stronger than the intensity of zero-phonon line of this centre at ambient pressure. We conclude that in this case the centre of inversion of the A centre is conserved, so the zero-phonon transitions are weaker than its vibronic sideband. Therefore the A centre environments are due to Ca²⁺ ions situated at the least in the position of second cation neighbours of the Mn⁴⁺ ions or farther. Thus the distance between the Mn⁴⁺ and the second neighbour is equal to at least 5.57 Å. In contrast to that in the B centre environment the Ca²⁺ ions are situated in the position of first neighbours at a distance of 3.47 Å from the central Mn⁴⁺.

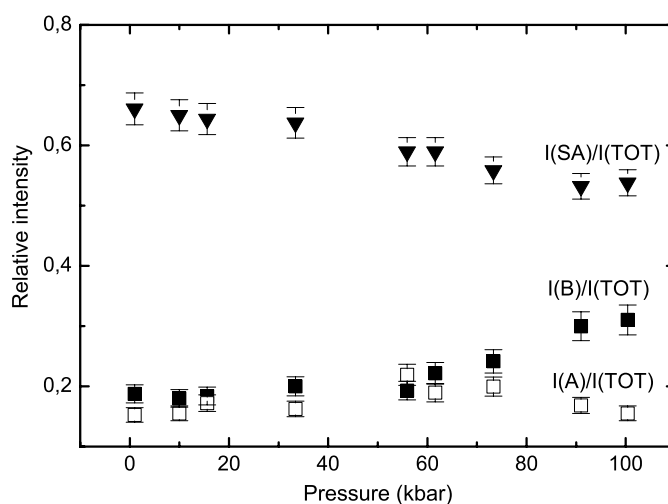


Figure 4. The pressure dependences of the integrated intensity ratio of the R_A and R_B lines and sideband of the R_A line (SA) to the total luminescence intensity in GGG:Mn⁴⁺ crystal, excited by the 514.5 nm argon-ion laser line at $T = 15$ K.

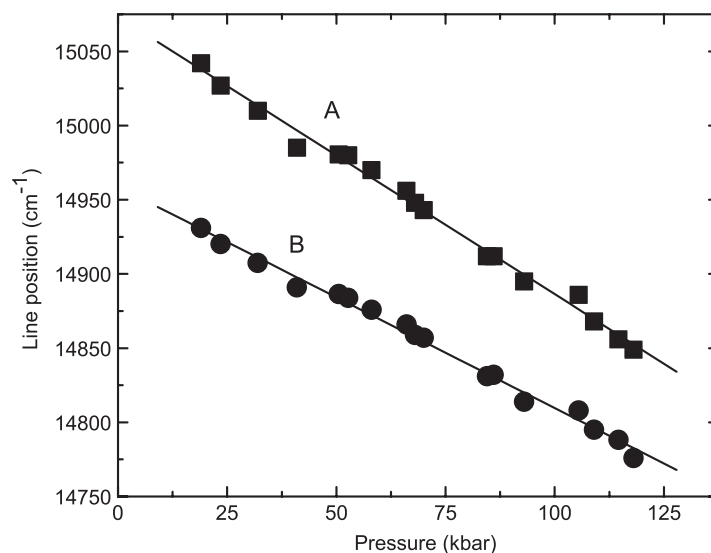


Figure 5. The pressure dependence energy of the R-lines for the A and B Mn⁴⁺ centres at $T = 15$ K. The lines are computer fits of the nephelauxetic effect model (see the text).

The emission spectrum of GGG:Mn⁴⁺ depends strongly on the excitation energy and the change of pressure. One can conclude that the absorption spectrum in the spectral region of the argon-ion laser line used for luminescence excitation must strongly shift with the pressure change in accordance with the energy structure of the d³ ion, predicted by the Tanabe–Sugano diagrams. Application of pressure strongly increases the energy of the ⁴A₂ → ⁴T₂ and the ⁴A₂ → ⁴T₁ transitions, that are strongly coupled to the lattice. The intensity dependences of the R-lines of the A and B centres (figure 4) additionally confirm this conclusion.

In the A site case at ambient pressure the zero-phonon transitions are weaker than its vibronic sideband. When the pressure increases, the intensity of R_A line increases relative to

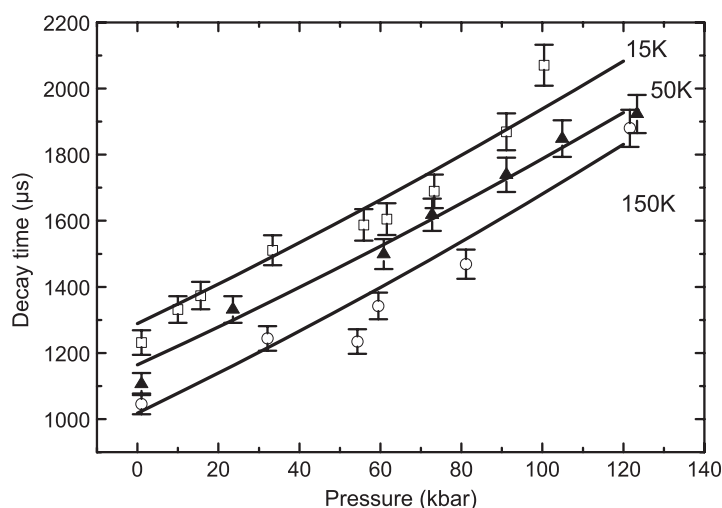


Figure 6. Pressure dependence of the luminescence decay times of the A centre of Mn^{4+} ions in GGG at $T = 15, 50$ and 100 K. The symbols are experimental data; the lines are computer fits.

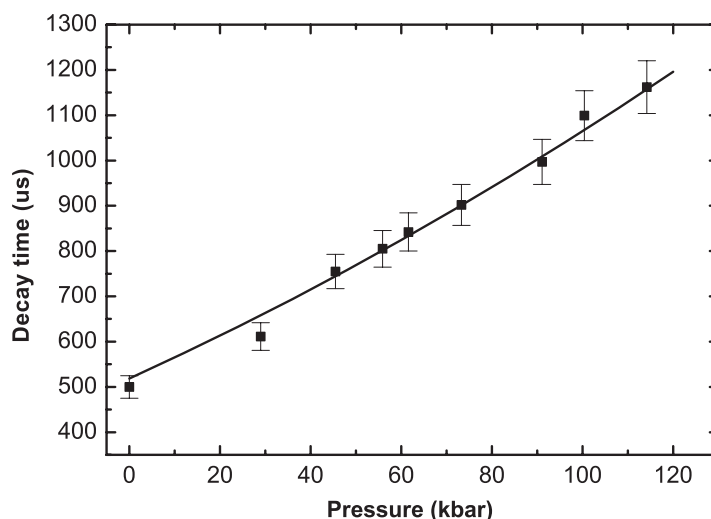


Figure 7. Pressure dependence of the luminescence decay times of the B centre of Mn^{4+} ions in GGG at $T = 15$ K. The symbols are experimental data; the line is a computer fit.

its sideband intensity (see figure 4). We conclude that the A site environments becomes more strongly perturbed at increased pressure. The centre of inversion is destroyed and the zero-phonon transitions becomes electric-dipole allowed and stronger than their phonon sideband.

The ${}^2\text{E}$ level is the first excited state for both A and B Mn^{4+} centres. The second excited level is ${}^4\text{T}_2$ level. These levels are coupled by the spin-orbit interaction. At elevated temperatures they can be additionally thermally coupled.

As a consequence of thermal and spin-orbit coupling, the properties of the first excited state of Mn^{4+} reflect a combination of the properties of both the ${}^2\text{E}$ and ${}^4\text{T}_2$ levels. Since emission from the ${}^2\text{E}$ state is spin forbidden, its lifetime is strongly influenced by admixing

with ⁴T₂ level. The reduction in spin–orbit coupling due to the shift of the ⁴T₁ excited level towards higher energies with increasing pressure leads to reduction in the mixing of the ²E and ⁴T₂ states. Thus increase of pressure causes an increase of the lifetime of the luminescence of the ²E state, which is seen in figures 6 and 7.

The pressure dependence of the luminescence decay kinetics can be modelled by considering the energetic structure of the Mn⁴⁺ ion, which consists of Γ₈(⁴A₂) ground and the Γ₈(⁴T₂), Γ'₈(⁴T₂), Γ₇(⁴T₂), Γ₆(⁴T₂), Γ₈(²E), Γ₈(²T₁), and Γ₆(²T₁) excited electronic manifolds mixed by the spin–orbit interaction. Since the Γ₈(⁴A₂) ground state is energetically well separated, we have omitted its coupling with the excited states.

We have considered the total Hamiltonian of the system given as a sum of the electronic Hamiltonian— H_e , lattice Hamiltonian— H_l , and electron–lattice interaction Hamiltonian— H_{e-l} ,

$$H(q, Q) = H_e(q) + H_l(Q) + H_{e-l}(q, Q). \quad (1)$$

Here q and Q are the electronic and configuration coordinates, respectively. The details of this Hamiltonian for the case Mn⁴⁺ and equivalent systems were discussed elsewhere (Grinberg 1993, Koepke *et al* 1998, Grinberg *et al* 1999). We have solved the problem using the diabatic representation (Grinberg *et al* 1993), where the electronic parts of the wavefunctions have been assumed to be independent of ionic positions. Thus the following Born–Oppenheimer functions represent the diabatic basis:

$$\psi_{\Gamma}^n(q, Q, s) = \varphi_{\Gamma}(q, s)\chi_{\Gamma}^n(Q) \quad (2)$$

where $\varphi_{\Gamma}(q, s)$ and $\chi_{\Gamma}^n(Q)$ are the electronic and ionic parts of the wavefunctions, respectively; $s = 1/2$ or $3/2$ represents the spin quantum number for doublet and quartet states, respectively, and n is the vibrational quantum number. According to the above assumptions, the electronic part of the Hamiltonian is the strong crystal-field Hamiltonian. Assuming the octahedral symmetry of the Mn⁴⁺ site, Γ corresponds to the irreducible representations of the double point group O_h. The vibronic part of the Hamiltonian describes the vibrations of the ligands. Although we have found that the ion motion is confined, we have used the harmonic approximation for consideration of the vibronic states related to each electronic manifold. This has been done for convenience since in the harmonic approximation the vibronic overlap integrals can be easily calculated by Manneback recurrence formulae (Manneback 1951).

We have considered the coupling only to the fully symmetrical breathing mode. Thus the harmonic approximation the electronic energies, parametrically dependent on ionic positions and the lattice vibration potentials, are given by the following parabolas:

$$\varepsilon_{\Gamma}(Q) = \varepsilon_{\Gamma}^0 + S_{\Gamma}\hbar\omega + \hbar\omega\frac{Q^2}{2} + \sqrt{2S_{\Gamma}}\hbar\omega Q \quad (3)$$

where S_{Γ} is the Huang–Rhys parameter of state Γ . S_{Γ} is assumed to be zero for all states belonging to the ground electronic configuration (all components of the ⁴A₂, ²E and ⁴T₁ electronic manifolds).

To calculate the energetic structure of the system, we have taken into account 50 vibronic states related to each electronic manifold. In such a way, we have created the Hamiltonian, where the diagonal matrix elements were defined by

$$H_{\Gamma\Gamma}^{nn} = \varepsilon_{\Gamma}^0 + H_{s-o}^{\Gamma\Gamma} + \left(n + \frac{1}{2}\right)\hbar\omega \quad (4)$$

where $H_{s-o}^{\Gamma\Gamma}$ are the spin–orbit matrix elements. The spin–orbit interaction is taken into account by the diagonal as well as by the off-diagonal part of the Hamiltonian. Actually in the diabatic representation, the off-diagonal part of the Hamiltonian is given only by the spin–orbit interaction. Considering the lattice vibrations and electron–lattice coupling, one

Table 1. Spin-orbit matrix elements (in ξ units).

| $H_{s-o}(\xi)$ | $\Gamma_8(^4T_2)$ | $\Gamma'_8(^4T_2)$ | $\Gamma_8(^2E)$ | $\Gamma_8(^2T_1)$ | $\Gamma_6(^4T_2)$ | $\Gamma_6(^2T_1)$ | $\Gamma_7(^4T_2)$ |
|--------------------|-------------------|--------------------|-----------------|-------------------|-------------------|-------------------|-------------------|
| $\Gamma_8(^4T_2)$ | -1/6 | 0 | $\sqrt{30}/15$ | $-\sqrt{5}/10$ | 0 | 0 | 0 |
| $\Gamma'_8(^4T_2)$ | | 1/4 | $\sqrt{30}/5$ | $\sqrt{5}/5$ | 0 | 0 | 0 |
| $\Gamma_8(^2E)$ | | | 0 | 0 | 0 | 0 | 0 |
| $\Gamma_8(^2T_1)$ | | | | 0 | 0 | 0 | 0 |
| $\Gamma_6(^4T_2)$ | | | | | 1/4 | $\sqrt{2}/2$ | 0 |
| $\Gamma_6(^2T_1)$ | | | | | | 0 | 0 |
| $\Gamma_7(^4T_2)$ | | | | | | | -5/12 |

obtains that the spin-orbit interaction is moderated by the vibronic overlap integrals. Thus the off-diagonal part of the Hamiltonian is given by

$$H_{\Gamma\Gamma'}^{nm} = H_{s-o}^{\Gamma\Gamma'} \int \chi_{\Gamma}^{n*}(Q) \chi_{\Gamma'}^m(Q) dQ. \quad (5)$$

The spin-orbit matrix elements, $H_{s-o}^{\Gamma\Gamma'}$, are listed in table 1.

Diagonalization of the Hamiltonian given by equations (4) and (5) allows us to calculate the vibronic energies as well as the wavefunctions of the system. The resulting states are characterized only by the single quantum number k , which is related to the energy E^k . The respective wavefunction is a mixture of all considered states and is given by the following superposition:

$$\Phi^k(q, Q) = \sum_{jm} a_j^{km} \left(\frac{1}{2}\right) \varphi_j(q, \frac{1}{2}) \chi_j^m(Q) + \sum_{in} a_i^{kn} \left(\frac{3}{2}\right) \varphi_i(q, \frac{3}{2}) \chi_i^n(Q). \quad (6)$$

Here the first and second sum represent the doublet and quartet contributions; $a_i^{kn} \left(\frac{3}{2}\right)$, $a_j^{km} \left(\frac{1}{2}\right)$ are coefficients obtained in the framework of the diagonalization procedure. Since the ground electronic manifold is the 4A_2 quartet, only the transition from the quartet excited states contribute to the luminescence. One calculates the contribution related to the transition from the $\Phi^k(q, Q)$ state to the l th vibronic state of the ground electronic manifold 4A_2 as follows:

$$I_{kl} = \sum_i \left| \int \varphi_{4A_2} \left(q, \frac{3}{2}\right) M(q) \varphi_i^* \left(q, \frac{3}{2}\right) dq \sum_n a_i^{kn} \left(\frac{3}{2}\right) \int (\chi_{4A_2}^l(Q) (\chi_i^n(Q))^* dQ \right|^2 n_i \quad (7)$$

where n_i is the degeneration of the states, which is 4 for Γ_8 and Γ'_8 , and 2 for Γ_6 and Γ_7 .

The quantity $\varphi_{4A_2} \left(q, \frac{3}{2}\right) M(q) \varphi_i^* \left(q, \frac{3}{2}\right) dq$ is the electronic transition moment. Since we have not considered a polarization, we have assumed that this quantity is the same for all quartet components. In such a way, the intensity of the transitions between the k th excited state and the l th vibronic state of the ground electronic manifold is proportional to the following sum of the vibronic overlap integrals:

$$I_{kl} \propto \sum_i \sum_l \left| a_i^{kn} \left(\frac{3}{2}\right) \int (\chi_{4A_2}^l(Q) (\chi_i^n(Q))^* dQ \right|^2 n_i. \quad (8)$$

Using our model, one can reproduce an energetic structure of a particular Mn^{4+} site and its luminescence decay time as a function of temperature and pressure.

One can calculate the luminescence decay time, τ . Considering that the luminescence lifetime is related to the radiative transition probability, P , by the relation $\tau = P^{-1}$ and the radiative transition probability is proportional to the emission intensity, one obtains

$$\tau^{-1}(E_{4T_2}, E_{2E}, T) = \frac{1}{\tau_0} \sum_k \sum_l I_{kl}(E_{4T_2}, E_{2E}) S[(E^k - E^0)/kT] \quad (9)$$

Table 2. Parameters of the Mn⁴⁺ sites in GGG. The values of the energy levels ⁴T₂ and ²E are given for ambient pressure at $T = 15$ K.

| Mn ⁴⁺ site | $E(^4T_2)$ (cm ⁻¹) | $dE(^4T_2)/dp$ (cm ⁻¹ kbar ⁻¹) | $E(^2E)$ (cm ⁻¹) | $dE(^2E)/dp$ (cm ⁻¹ kbar ⁻¹) | Spin-orbit parameter ξ | $Sh\omega$ (cm ⁻¹) | $h\omega$ (cm ⁻¹) |
|-----------------------|-----------------------------------|--|---------------------------------|--|-------------------------------|-----------------------------------|----------------------------------|
| A | 19 300 | 13 | 15 070 | -1.9 | 300 | 2600 | 360 |
| B | 19 700 | 18 | 14 970 | -1.5 | 300 | 2600 | 360 |

where $I_{ki}(E_{4T_2}, E_{2E})$ is given by equation (7). τ_0 is the time constant that represents the pure quartet lifetime and is related to the transitions moment as follows:

$$\tau_0^{-1} = \left| \int (\varphi_{4A_2}^*)(q, \frac{3}{2}) M(q) (\varphi_{4T_2})(q, \frac{3}{2}) dq \right|^2. \quad (10)$$

Equation (9) results in the dependence of the luminescence decay time on the energetic structure of manganese ion.

This theory was already presented in Kaminska *et al* (2000). Since in this reference some typographical errors appeared, we take this opportunity to correct them. Also we present here the application of this theory for a description of the pressure dependence of the luminescence decay times at elevated temperatures, which was not done in Kaminska *et al* (2000).

As input parameters the model uses specific energies of the ⁴T₂ and ²E electronic manifolds of the total Hamiltonian at ambient pressure; the pressure coefficients $dE(^4T_2)/dp$ and $dE(^2E)/dp$ for the energies of the ⁴T₂ and ²E states, respectively; the value of the spin-orbit interaction parameter ξ ; the energy of fully symmetrical phonon coupled with ⁴T₂ state; the Huang-Rhys coupling factor S ; and the value of the decay time of the ⁴T₂ \rightarrow ⁴A₂, τ_0 . Some of those parameters are known from experiments (the pressure coefficients, decay times), or from earlier calculations; the others are treated as adjustable parameters for the computer fits. From the fits the values of the Huang-Rhys coupling constant, the spin-orbit interaction parameter and the phonon energy are obtained. We have assumed that the spin-orbit interaction, the electron lattice coupling energy and the phonon energy do not depend on the pressure. These assumptions are in good agreement with real experimental conditions.

The experimental pressure dependences of the luminescence decay are expressed by equation (9). The calculations were performed for the two observed Mn⁴⁺ centres A and B, respectively. The results are shown as in figures 6 and 7.

Reasonable good agreement of the model with data for both A and B centres is observed. The parameters of the fit are presented in table 2.

The values of the effective phonon energy $h\omega$ are in very good agreement with the energy of the dominating phonon in the Raman spectrum of the GGG:(Mn, Ca) crystals (Brenier *et al* 1992). The spectral positions of the ⁴T₂ bands also agree very well with those established from the photoluminescence excitation measurements (Brenier *et al* 1992). The obtained value of $Sh\omega$ is relatively large. Maybe this is due to magnetic interaction between Mn⁴⁺ and Gd³⁺ ions. That may also be caused by strongly perturbed octahedral symmetry of the investigated sites.

4.2. Nephelauxetic effect in the luminescence of Mn⁴⁺ ions in GGG crystals

The decrease of the energy of the ²E \rightarrow ⁴A₂ transitions (R-lines) with increase of pressure is a fingerprint of the nephelauxetic effect, i.e. decrease of the values of the B and C Racah parameters due to the covalency of bonds. Pressure application increases the covalency effects due to decrease of the metal-ligand distances. Recently, we proposed a model that explains

quantitatively the nephelauxetic effect in the framework of the Harrison theory of covalent–ionic bonding (Biernacki *et al* 2002). The model is especially useful for describing the pressure dependence of the effect. According to that model the B , C and Dq Racah parameters are pressure scaled with the use of the Murnaghan equation and a polarity parameter a , equal to

$$a = \frac{V_3}{\sqrt{V_2^2 + V_3^2}} \quad (11)$$

where the covalent energy $V_2 = \eta h^2/mR_0^2$, m is the electron mass and the dimensionless coefficient η will be treated as an adjustable parameter in further calculations. $V_3 = (\varepsilon_s - \varepsilon_p)/2$ is the polar energy. The ε_s and ε_p are the values of Hartree–Fock energies of the s states of cation and p states of oxygen, which participate in bonding. The bulk modulus and its pressure derivative of the material studied are also the parameters of the model through the Murnaghan equation (Murnaghan 1944).

The results of the computer fit of the model to the data are presented in figure 5 as solid lines. The values of the fitting parameter of the model, η , are equal to 3.57 and 2.55 for the A and B centre, respectively. We consider the fits obtained as excellent.

The experimental values of the pressure coefficients of the 2E state of various Mn^{4+} centres in GGG are about three times larger than those for Cr^{3+} ions (Hommerich and Bray 1995), which have the same electronic structure of the outer shell (d^3). This effect may be partially explained by stronger covalency of bonds between Mn^{4+} and O^{2-} ions due to stronger Coulomb interaction than for Cr^{3+} ions. In addition, stronger interaction between Mn^{4+} and the host Gd^{3+} ions, mediated through oxygen, may be also the reason for the larger value of the pressure coefficient. The Hartree–Fock energies for the 3d levels of the neutral atoms (Froese 1972) are the following: Cr—1.13 Ryd, Mn—1.27 Ryd. The energies of the other levels of interest are: Gd (4f)—1.51 Ryd, and O(2p)—1.26 Ryd. In the GGG garnet the 2p levels are split into a broad p band due to interaction with Gd and Ga atoms. Since Mn enters the GGG host in a higher oxidation state than Cr its 3d levels are additionally lowered by the Coulomb attraction and they have comparable values with the 4f levels of Gd. Mn^{4+} and Gd^{3+} ions are coupled via intervening oxygen ions, which in the 2-charge state have large ionic radii of 1.32 Å. Having similar energies, the 4f electrons of Gd^{3+} and 3d electrons of Mn (being in resonance with the oxygen valence band) strongly interact electrostatically. Due to this also magnetic interactions in Mn^{4+} -doped GGG are stronger than those observed for GGG: Cr^{3+} ions (Suchocki *et al* 2004).

5. Conclusions

The effect of pressure on the luminescence properties of Mn^{4+} :GGG crystals has been studied. Interesting comparisons can then be made with analogous Cr^{3+} :GGG spectra. The red shift of the R-lines is associated with the so-called nephelauxetic effect, related to change of interelectronic repulsion of the d-electrons due to the increased covalency of the central ion–oxygen bonds with increased pressure. Much larger value of the pressure coefficient observed for the Mn^{4+} ion in GGG in comparison with the Cr^{3+} can be explained by the different strength of coupling of these both isoelectronic ions with the GGG host. High hydrostatic pressure changes the strength of the coupling of the 2E and 4T_2 states, which strongly affects the radiative decay probability of the 2E state. A theory was presented that quantitatively explains the dependence of the luminescence lifetime on pressure and temperature. The obtained agreement between theory and experimental data is very good. This work demonstrates that high pressure is capable of tuning important optical properties of solid-state laser materials.

Acknowledgment

This work was partially supported by of the Polish Committee for Scientific Research during the years 2001–2006.

References

- Biernacki S W, Kamińska A, Suchocki A and Arizmendi L 2002 *Appl. Phys. Lett.* **81** 442
- Brenier A, Suchocki A, Pedrini C, Boulon G and Madej C 1992 *Phys. Rev. B* **46** 3219
- Donegan J F, Glynn T J, Imbusch G F and Remeika J P 1986 *J. Lumin.* **36** 93
- Dong J and Lu K 1991 *Phys. Rev. B* **43** 8808
- Froese Ch 1972 *Atomic Data* vol 4, p 301
- Geschwind S, Kisliuk P, Klein M P, Remeika J P and Wood D L 1962 *Phys. Rev.* **126** 1684
- Grinberg M 1993 *J. Lumin.* **54** 369
- Grinberg M, Felici A C, Papa T and Piacentini M 1999 *Phys. Rev. B* **60** 8595
- Grinberg M, Macfarlane P J, Henderson B and Holliday K 1995 *Phys. Rev. B* **52** 3912
- Grinberg M, Mandelis A and Fjedsted F 1993 *Phys. Rev. B* **48** 5935
- Grinberg M and Orlikowski T 1992 *J. Lumin.* **53** 447
- Hazenkamp M F, Gudel H U, Kuck S, Huber G, Rauw W and Reinen D 1997 *Chem. Phys. Lett.* **265** 264
- Hernandez, Rodriguez F, Moreno M and Gudel H U 1999 *Physica B* **265** 186
- Hommerich U and Bray K L 1995 *Phys. Rev. B* **51** 12133
- Hong H, Mirov S and Vohra Yogesh K 1996 *Phys. Rev. B* **54** 6200
- Jovanić B R 1997 *J. Lumin.* **75** 171
- Kaminska A, Suchocki A, Grinberg M, Arizmendi L, Callejo D and Jaque F 2000 *Phys. Rev. B* **62** 10802
- Koepke Cz, Wiśniewski K, Grinberg M, Russell D L L, Holliday K and Beall G H 1998 *J. Lumin.* **78** 135
- Loutts G B, Warren M, Taylor L, Rakhimov R R, Ries H R and Miller G III 1988 *Phys. Rev. B* **57** 3706
- Manneback C 1951 *Physica* **117** 1001
- Moncorge R, Manaa H and Boulon G 1994 *Opt. Mater.* **4** 139
- Murnaghan F D 1944 *Proc. Natl Acad. Sci.* **30** 244
- Noack R A and Holzapfel W B 1976 *High Pressure Science and Technology* vol 1, ed K D Timmerhaus and M S Barber (New York: Plenum) p 748
- Piermarini G J, Block S, Barnett J D and Forman R A 1975 *J. Appl. Phys.* **46** 2774
- Stoyanova R, Gorova M and Zheckeva E 2000 *J. Phys. Chem. Solids* **61** 609
- Sturve B and Huber G 1985 *Appl. Phys. B* **36** 195
- Suchocki A, Allen J D and Powell R C 1986 *Phys. Rev. B* **36** 6729
- Suchocki A, Biernacki S W, Boulon G, Brenner A, Potemski M and Wyszomolek A 2004 *Chem. Phys.* **298** 267–72
- Sugano S, Tanabe Y and Kamimura M 1970 *Multiplets of Transition-Metal Ions in Crystals* (New York: Academic)
- Zheng W-C 1999 *J. Phys. Chem. Solids* **60** 359